Particle Size Distribution of Gas Metal and Flux Cored Arc Welding Fumes

Impactor separation of welding fumes shows at least two size modes, the relative magnitude of which is determined by the welding process

BY N. T. JENKINS, W. M.–G. PIERCE, AND T. W. EAGAR

ABSTRACT. A cascade impactor was employed to separate the fume particles in order to determine the size distribution of welding fume. Clear images of coarse welding fume particles (microspatter) from scanning electron microscopy are presented. The particle size distribution of the welding fume reveals that gas metal arc welding (GMAW) fume consists predominately of particle agglomerates smaller than approximately one micrometer. Less than 10% of the fume by weight is microspatter, which is larger than a micrometer. This fraction of microspatter does not change greatly as the GMAW parameters are changed. Flux cored arc welding (FCAW) fume contains more microspatter, approximately 30% by weight.

Introduction

Arc welding poses many hazards, including heat, noise, vibration, and electricity. Radiation from the arc can cause eye and skin damage. Gases and respirable particles in the welding environment contain chemicals that can create adverse side effects after inhalation, if delivered in the appropriate dose and chemical state. A major source of respirable particles is welding fume.

Aerosol scientists use the term "fume" to describe any airborne metal or metal oxide particles that condense from vapor (Ref. 1), which is indeed the case for most particles formed from welding. However, some airborne particles generated by welding are not formed from vapor condensation, but from liquid droplet ejection, and thus are not technically fume particles. Welding spatter is formed from liquid droplets and is for the most part too large to remain airborne; droplets small enough to remain airborne have been termed microspatter. The welding community has traditionally labeled all airborne particles formed during welding as "welding fume," including microspatter, despite it not technically being fume. This naming convention is used here.

Particles smaller than 20 μm in diameter can remain airborne (Ref. 2), but not all airborne particles are deposited the same way in the lungs, because airborne particles of different sizes behave differently aerodynamically. Objects greater than a few micrometers in size are trapped on the walls of the human airway before they reach the lungs. They are carried away in the mucus, which is then transported to the digestive tract. Particles smaller than 0.1 μm are inhaled and deposited in the lungs. The path of entry into the body strongly affects the biological fate of the chemicals present in the inhaled particles. Particles or agglomerates between 0.1 and 1 μm can be exhaled, meaning that only about 30% of particles of this size eventually deposit in the lungs (Ref. 3). Therefore, it is important to measure the size distribution of particles in order to ascertain the respirable fraction thereof.

Zimmer and Biswas (Ref. 4) reported the results of using two different airborne particle counters with different size range capabilities to measure the particle size of gas metal arc welding (GMAW) fume. This provided a particle size distribution over all sizes of interest. Three modes of particle sizes can clearly be distinguished: a nucleation mode of individual particles from a few nanometers to ~0.1 μm, an accumulation mode (~0.1 to ~1 μm) of agglomerated, aggregated, and coalesced particles formed from the nucleation mode, and a coarse mode of unagglomerated particles in the range of ~1 to ~20 μm.

Particles in the nucleation mode form by vapor condensation. Because particles in the accumulation mode agglomerate from nucleation mode particles, vapor chemistry also controls accumulation particle composition. The particles formed from nucleation are called primary particles whenever found in fractal-like agglomerates or aggregates. Aggregates refer to clumps of primary particles that have fused together. Agglomerates are those particles made up of primary particles that adhere together because of electrostatic or van der Waals forces. The nucleation and accumulation modes are therefore often grouped together as "fine particles," which distinguishes them from the coarse mode particles created through liquid ejection (Ref. 5).

Coarse particles, or microspatter, in welding fume have been reported earlier (Ref. 6). Because the median diameter of coarse particles is an order of magnitude larger than the median diameter of agglomerates (Ref. 2), coarse particles may presumably dominate the bulk chemistry of welding fume, even if these coarse particles are few in number.

There seems to be a correlation between fume formation rate (FFR) and spatter formation rate. Some researchers (Refs. 6, 7) have proposed that the formation of additional microspatter explains why processes that create more spatter, such as globular GMAW or flux cored arc welding, have greater fume formation rates. A comparison of the particle size distributions of various welding processes would yield insight into how welding fume forms, which would help determine which process controls are most effective in reducing fume formation.

Several studies on the size of welding

KEYWORDS

Airborne Particles
Arc Welding
Flux Cored Arc Welding
Fumes
Gas Metal Arc Welding
Particulate
Welding Fume

N. T. JENKINS is with the College of Medicine, The Ohio State University, Columbus, Ohio. W. M.–G. PIERCE is with the College of Medicine, Drexel University, Philadelphia, Pa. T. W. EAGAR is with the Department of Materials Science and Engineering, Massachusetts Institute of Technology, Cambridge, Mass.

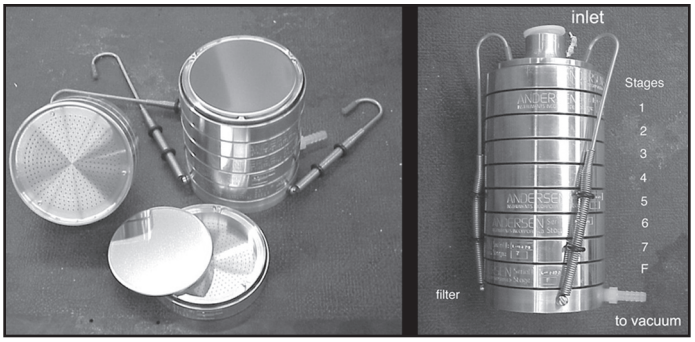

Fig. 1 — Andersen cascade impactor. Only stages 1, 5, 6, and F, and the bottom filter were used.

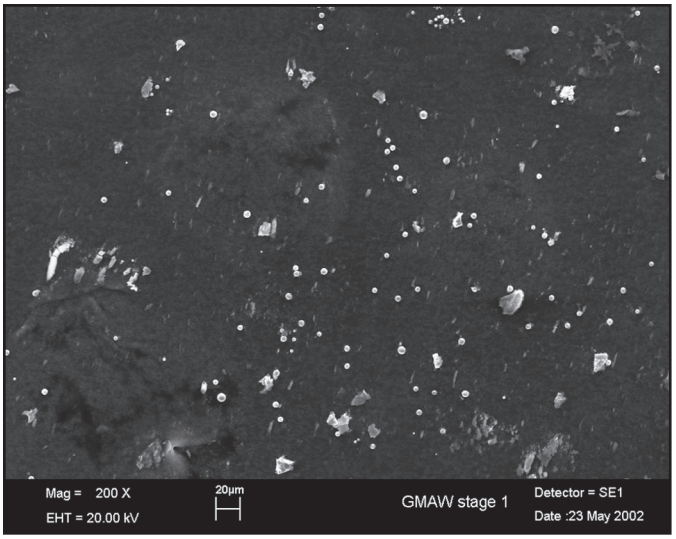

Fig. 2 — Scanning electron microscopy of stainless steel GMAW fume particles collected with a cascade impactor on stage 1, designed to capture particles with $d_{aerodynamic} > 5.8$ µm. The count median diameter (CMD) of these particles is 5.0 µm with a geometric standard deviation (σ_g) of 1.7.

fume have previously been reported. Researchers have measured the size distribution of welding fume with impactors (Refs. 3, 8–13), and with airborne particle counters (Refs. 4, 12, 14–16). Because of the large size range of particles, no single technique can measure the size of every particle. Only expensive impactors can distinguish between particles smaller than 0.1 µm. Airborne particle counters (e.g., laser particle counter or electric aerosol analyzer) are only effective in a limited size range; most do not detect particles larger than 2 µm. In addition, there are concerns that airborne particle counters may not measure the true particle diameter for welding fume (Ref. 17). Optical particle counters detect particle light scattering, which is determined by particle shape and refraction index. Particles can be counted while airborne by measuring electric mobility, which is strongly dependent on the surface area of the particles. Since welding fume particles are primarily fractal-shaped agglomerates with complex and nonuniform shapes and surfaces, it is difficult to calibrate such measurement techniques to welding fume with standards established with spherical particles.

Impactors separate particles by aerodynamic diameter ($d_{aerodynamic}$), which is not necessarily the true particle diameter. However, the $d_{aerodynamic}$ is the particle property that determines inhalation and lung deposition. Unlike airborne particle counters, an impactor can be used to divide welding fume into size groups that then can be examined separately in a scanning electron microscope (SEM). Without such size separation, it is difficult to resolve useful images of welding fume in a SEM because the fume otherwise clumps in indistinguishable masses. The size groups separated by impaction can also be analyzed chemically in order to characterize the compositional dependence of particle size (Ref. 18).

In this paper, a cascade impactor was used to separate welding fume into size groups for analysis. Although the impactor used could not distinguish between particles in the nucleation mode and accumulation mode, it was able to collectively separate these two groups of fine particles from the coarse particles. The mass distribution found with cascade impaction can be used to determine whether spatter contributes to welding fumeformation and help determine how fume is inhaled.

Methods and Results

Fume was created by arc welding in a fume chamber described elsewhere (Ref. 7). Four different methods were employed: gas metal arc welding with three different sets of parameters and correspondingly different metal transfer modes (globular, spray, and pulsed), and one type of self-shielded flux cored arc welding (Table 1).

A cascade impactor (Thermo Andersen Nonviable Eight Stage Cascade Im-

Table 1 — Description of Welding Processes Used to Create Fume Studied

Welding Process	Shield Gas	Electrode AWS Designation	Current (amp)	Voltage (volt)	Wire Speed (ipm) (mm/s)	Pulse Width (ms)
Globular GMAW	2%O_2-Ar	ER308L 0.045 in.	~130	30	180 (76)	NA
Spray GMAW	2%O_2-Ar	ER308L 0.045 in.	~185	30	300 (127)	NA
Pulsed GMAW	2%O_2-Ar	ER308L 0.045 in.	peak:-325 ave:-100	average: ~30 background:19	180 (76)	2.8
FCAW	none	ER308FC-0 0.045 in.	~170	30	530 (224)	NA

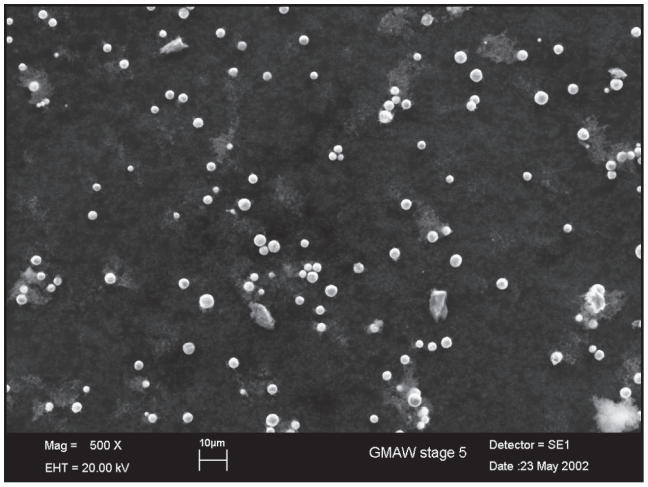

Fig. 3 — Scanning electron microscopy of stainless steel GMAW fume particles collected with a cascade impactor onto stage 5, designed to capture particles with 1.1 µm < $d_{aerodynamic}$ < 5.8 µm. The count median diameter (CMD) of these particles is 3.7 µm with a geometric standard deviation (σ_g) of 1.5.

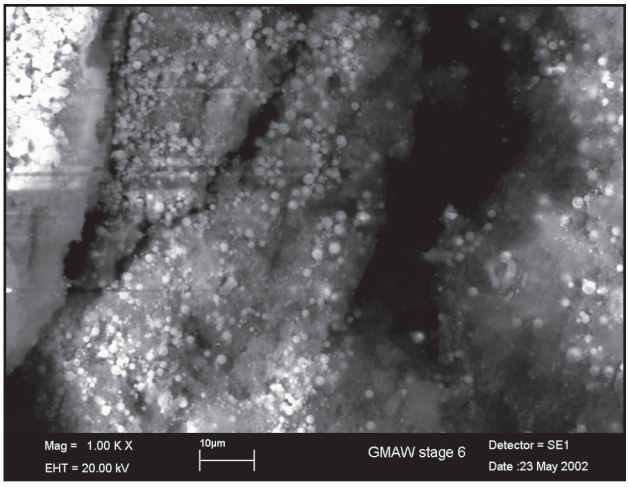

Fig. 4 — Scanning electron microscopy of stainless steel GMAW fume particles collected with a cascade impactor onto stage 6, designed to capture particles with 0.7µm < $d_{aerodynamic}$ < 1.1 µm. The count median diameter (CMD) of these particles is 0.7 µm with a geometric standard deviation (σ_g) of 1.9.

Table 2 — Mass Distribution (in milligrams) of Various Welding Fumes Measured with Cascade Impactor

		FCAW				globular GMAW			spray GMAW			pulsed GMAW		
Run		1	2	3	4	1	2	3	1	2	3	1	2	3
Sampling Time (s)		10	12	13	15	60	65	75	120	180	180	120	150	240
Stage	$d_{aerodynamic}$ (µm)	Mass (mg)												
1	>5.8	1.18	1.23	1.64	2.37	0.20	0.27	0.39	0.09	0.14	0.20	0.40	0.38	0.73
5	1.1 – 5.8	0.64	0.67	0.82	1.05	0.20	0.22	0.25	0.09	0.12	0.12	0.12	0.17	0.13
6	0.7 – 1.1	3.43	4.61	4.82	8.77	1.93	3.17	4.21	1.16	1.70	1.69	1.42	0.82	1.42
F	0.4 – 0.7	4.79	5.38	5.87	8.45	4.60	5.24	7.00	2.10	2.89	2.96	0.89	1.43	2.59
Filter	<0.4	9.21	10.95	13.4	16.64	24.71	26.18	31.29	20.68	31.04	31.24	15.06	19.33	31.17
Sum		19.25	22.84	26.55	37.28	31.64	35.08	43.14	24.12	35.89	36.21	17.89	22.13	36.04

pactor Series 20-800 Mark II, Fig. 1) was connected to the chimney of the fume chamber, with approximately 0.5 m between the welding arc and the impactor. The vacuum supplied with the impactor drew 28.3 L/min of air from the chamber into the impactor where airborne particles were collected at various stages onto impaction plates during welding. The plates from each stage were weighed before and after fume collection using a Mettler AE 163 microbalance with ± 50 µg precision. Before collection, a larger vacuum pulled air and fume out of the chamber to prevent buildup. It was turned off when the impactor vacuum was turned on. Collection times ranged from 10 s for FCAW to 4 min for pulsed GMAW and were sufficient to obtain adequate material to weigh, but care was also taken to collect no longer than necessary. Overloading on the impaction plates can cause some impacted particles to become reentrained in the airflow and to reimpact on the incorrect stage (Ref. 19).

The relative fume formation rate was determined by dividing the total mass collected in the cascade impactor by the collection time. The fume formation rate of globular GMAW was about 2.7 times greater than that of spray GMAW, which was in turn 1.4 times greater than pulsed GMAW; and FCAW formed fume at rates 10 times that of spray GMAW.

The airflow through an impactor is controlled by a jet plate in each stage so that particles impact on the corresponding collection plate according to their inertia. Therefore only particles with a small enough $d_{aerodynamic}$ can pass a given stage. This cutoff aerodynamic diameter is smaller for each successive stage. Therefore, the largest particles impact on the first plate and are removed from the air stream, then slightly smaller particles impact on the next plate, and so on. An oil or grease on the stages can be used to prevent particle bounce, if that is a concern. This was not done, because welding fume is known to adhere well to clean metal surfaces. At the final stage, a filter collects all particles with $d_{aerodynamic}$ smaller than a certain size.

Not all of the eight stages of the im-

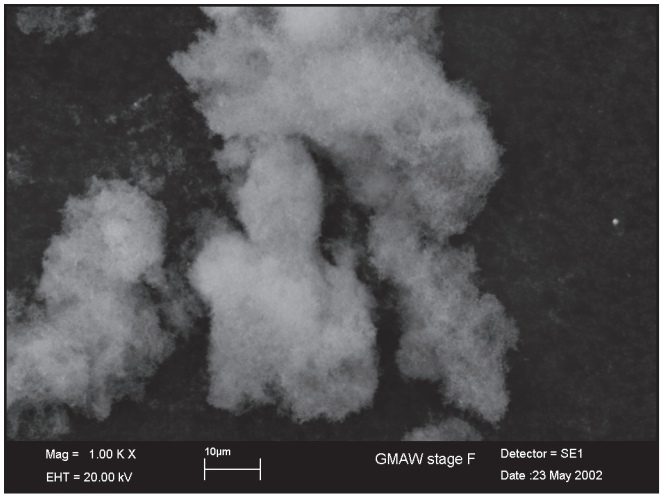

Fig. 5— Scanning electron microscopy of stainless steel GMAW fume particles collected with a cascade impactor onto stage F, designed to capture particles with 0.4 µm < $d_{aerodynamic}$ < 0.7 µm. No individual particles > 1 µm detected.

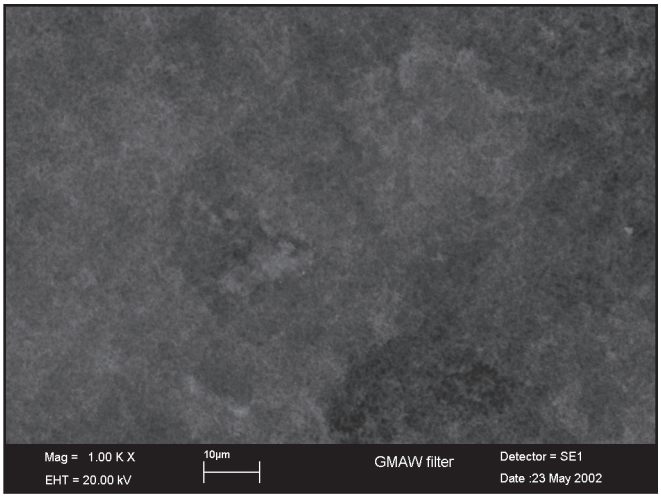

Fig. 6 — Scanning electron microscopy of stainless steel GMAW fume particles collected with a cascade impactor onto the filter, designed to capture particles with $d_{aerodynamic}$ < 0.4 µm. No individual particles > 0.5 µm detected.

Table 3 — Average Particle Size Distribution, by Percentage (%) of Total Fume Mass Collected

Impactor Stage	Aerodynamic Diameter	FCAW	Globular GMAW	Spray GMAW	Pulsed GMAW
1	>5.8	6.01	0.77	0.44	1.99
5	1.1 –5.8	3.04	0.61	0.35	0.60
6	0.7 – 1.1	19.9	8.30	4.74	5.19
F	0.4 – 0.7	23.3	15.2	8.31	6.21
Filter	<0.4	47.7	75.1	86.2	86.0

pactor were used in this study; according to the manufacturer, this does not change the aerodynamics of the remaining stages, which simply collect the particles that would have impacted on the missing stages.

The $d_{aerodynamic}$ is the equivalent diameter of a spherical particle with 1 g/cm^3 density with the same inertial properties as the particles in question. For spherical particles, the actual diameter can be found by dividing the aerodynamic diameter by the square root of the density of the particles (Ref. 2). If the density or particle shape is unknown, it is useful to directly measure the particle size collected at each impactor stage for each type of particulate material that is collected. This was done for GMAW fume created in spray mode and for FCAW fume.

Fume particles were transferred to adhesive SEM stubs by pressing the stubs against impaction plates after collection. Scanning electron micrographs of the stubs (Figs. 2–11) were analyzed on a Macintosh Powerbook G4 computer using the public domain *NIH Image* program (developed at the U.S. National Institutes of Health and available on the Internet at *http://rsb.info.nih.gov/nih-image/*) to determine the particle size collected on each plate. Because of the design of the impactor, many particles impacted in piles that made measurement of a single particle difficult. Care was taken to create micrographs only of regions where particle pileup did not occur. In addition, smaller welding fume particles often aggregate in the air before collection to form larger particle agglomerates that behave and impact like larger spherical particles. These agglomerates appear like foam or fine tangled hair in the micrographs (Figs. 5, 6, 10, 11). The effective particle diameter of an aggregate was calculated from the area of the two-dimensional image. However, the majority of the analyzed particles in the top three stages were individual spheres (or circles in the two-dimensional micrographs), so this approximation did not introduce substantial error into the measurement of those stages. At least 100 particles were measured per stage and a count median diameter (CMD) determined for each of the top three stages, along with the respective geometric standard deviation (σ_g). Individual fume particles smaller than approximately 0.5µm were difficult to resolve in the standard SEM used in the study. Agglomeration of these ultrafine particles also made resolution difficult. Therefore, only the approximate maximum particle size found is reported for the bottom two stages (stage F and the filter).

These data compared favorably to those obtained from measuring particles collected in the cascade impactor from iron powder with a known diameter dusted into the air. This iron powder was used to test the measurement technique because it was commercially prepared through liquid atomization and did not contain ultrafine particles to obscure the measurements.

As stated previously, the mass of each impaction plate was measured before and after collection. Fume collection and mea-

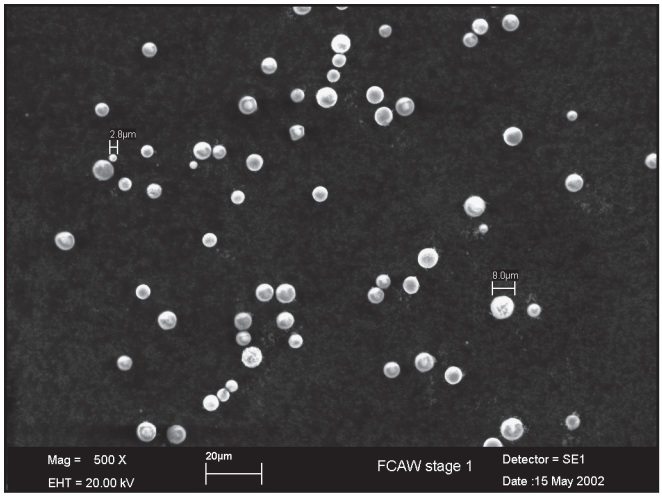

Fig. 7 — Scanning electron microscopy of stainless steel FCAW fume particles collected with a cascade impactor on stage 1, designed to capture particles with $d_{aerodynamic} > 5.8$ µm. The count median diameter (CMD) of these particles is 6.3 µm with a geometric standard deviation (σ_g) of 1.2.

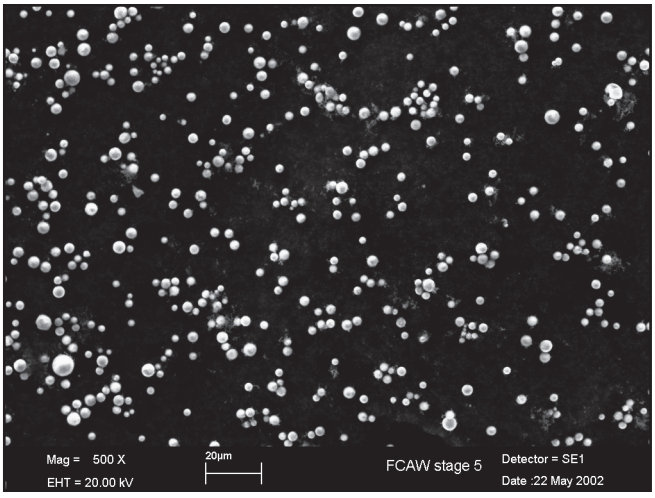

Fig. 8 — Scanning electron microscopy of stainless steel FCAW fume particles collected with a cascade impactor onto stage 5, designed to capture particles with 1.1 µm < $d_{aerodynamic}$ < 5.8 µm. The count median diameter (CMD) of these particles is 3.3 µm with a geometric standard deviation (σ_g) of 1.4.

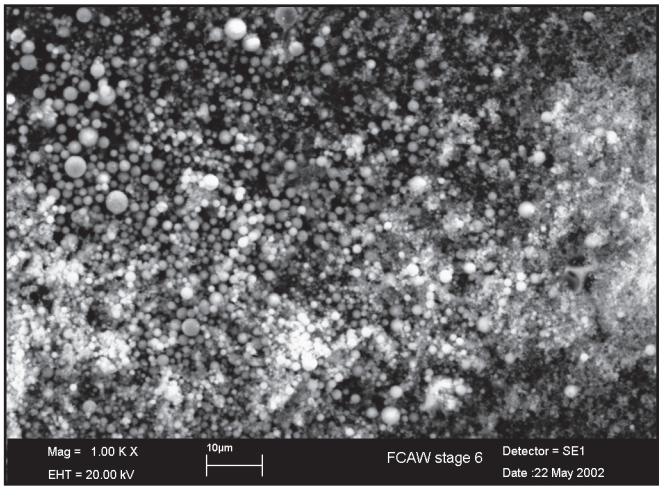

Fig. 9 — Scanning electron microscopy of stainless steel FCAW fume particles collected with a cascade impactor onto stage 6, designed to capture particles with 0.7 µm < $d_{aerodynamic}$ < 1.1 µm. The count median diameter (CMD) of these particles is 0.9 µm with a geometric standard deviation (σ_g) of 2.0.

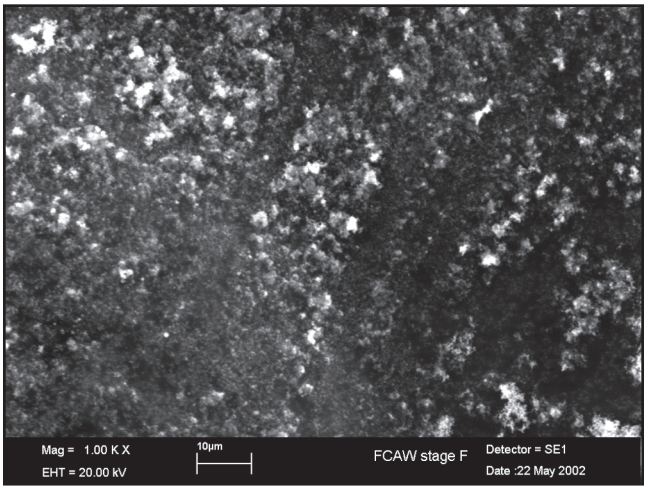

Fig. 10 — Scanning electron microscopy of stainless steel FCAW fume particles collected with a cascade impactor onto stage F, designed to capture particles with 0.4 µm < $d_{aerodynamic}$ < 0.7 µm. No individual particles > 1 µm detected.

surement were performed successfully three or four times for each fume type and then averaged. The resulting data are reported in Table 2.

The mass distribution data must be transformed for useful comparison between various welding fumes. One way to do this is by reporting the average distributions for each process as percentages of the total mass collected, as shown in Table 3.

The size distributions can also be plotted in a relative mass histogram with log-normal axes — Fig. 12. Two important points should be made about histograms of particle size distributions. First, the width of a histogram bin affects the total mass in each bin. To account for this, the mass should be divided by the width of the bin, which here is the logarithmic range in particle size collected by each impactor stage. This range is related to the second point: the lowest cutoff and highest cutoff for cascade impactors must sometimes be estimated in order to incorporate the data from the top and bottom stages into the histogram. For example, the top stage in the impactor used in this study collected all particles larger than 5.8 µm. To divide the mass from this stage by the range in particle size collected, one must estimate the effective upper cutoff to the particle size collected on the top stage. Only particles smaller than 20 µm remain airborne, so this was used for the upper cutoff. The largest particle found on the top stage with SEM was 18 µm, so this estimate is reasonable. The bottom stage in the impactor contains a filter that collects all particles smaller than 0.4 µm. The approximate size limit for the accumulation mode, 0.1 µm, was used as the lower cutoff estimate for the bottom stage. There are likely smaller welding fume particles in the air, but they would have accumulated into agglomerates upon deposition on the filter.

One can see that the accuracy of an impactor histogram can be dependent on certain estimates. A less error-prone method of reporting the data is with a cu-

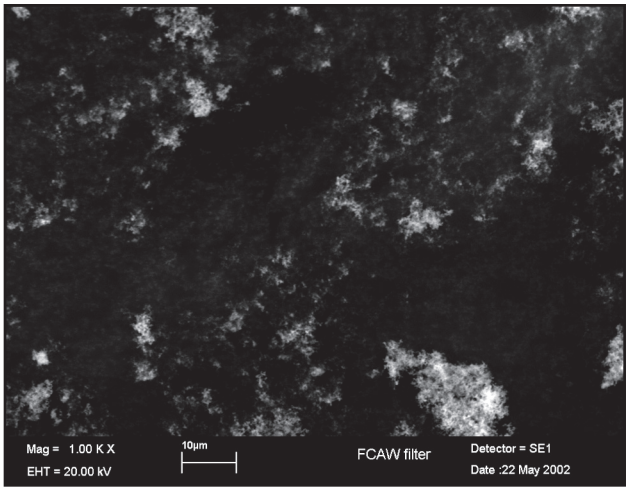

Fig. 11 — Scanning electron microscopy of stainless steel GMAW fume particles collected with a cascade impactor onto the filter, designed to capture particles with $d_{aerodynamic} < 0.4$ µm. No individual particles > 0.5 µm detected.

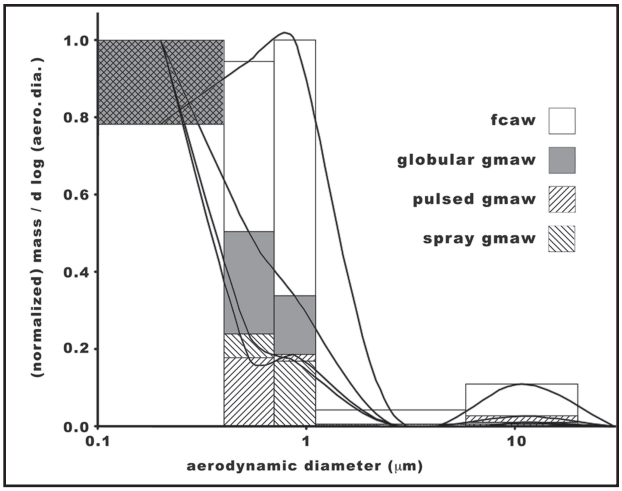

Fig. 12 — Relative mass histogram of welding fume particles captured with cascade impactor.

Table 4 — Overall Mass Median Aerodynamic Diameter (MMAD) and Geometric Standard Deviation (σ_g) of Welding Fume Particles Collected with Cascade Impactor

	FCAW		globular GMAW		spray GMAW		pulsed GMAW	
Mass Median Diameter (mm)	MMAD	σ_g	MMAD	σ_g	MMAD	σ_g	MMAD	σ_g
All Stages	0.33	4.0	0.07	5.8	0.02	7.9	0.04	8.2
	(SD = 0.03)		(SD = 0.001)		(SD = 0.02)		(SD = 0.001)	
Bottom Three Stages Only	0.43	1.4	0.33	1.5	0.25	1.6	0.24	1.7
(Accumulation Mode)	(SD = 0.003)		(SD=0.003)		(SD = 0.02)		(SD = 0.02)	
Top Two Stages Only	6.7	n.a.	6.1	n.a.	6.1	n.a	7.3	n.a
(Coarse Mode)	(SD = 0.06)		(SD = 0.3)		(SD = 0.3)		(SD = 0.5)	

Note: that the standard deviation (SD) is from comparison of MMADs of various runs, whereas σ_g is a measure of how the averaged data of a group of runs varies from the average MMAD of that group of runs.

mulative probability plot using probit versus linear axes — Fig. 13. Here one reports the percentage of total mass that is smaller than the upper cutoff size of each stage. The need for finding the lower cutoff for the bottom stage can thus be avoided. The only drawback to a probability plot is that it can be more difficult to see multiple size modes if present. However, it is easy to find the mean mass aerodynamic diameter (MMAD) on a cumulative probability plot. It is simply the intersection or extrapolation of the data through the 50th percentile. The MMAD along with the corresponding geometric standard deviation can be used as the descriptive values of the entire size distribution. See Table 4 for the MMADs of the various welding fumes.

Discussion

Berner and Berner (Ref. 10) noted that the welding fume particle size distribution that they measured could be explained with the trimodal model of atmospheric aerosols, because it was close to the logarithmic normal except for high concentrations at the tails.

The size distributions shown in Fig. 12 also seem to fit the trimodal model, although because of size limitations with the cascade impactor, no direct evidence of the nucleation mode is available. However, the coarse fraction is clearly distinct from the accumulation mode.

This can also be seen in the cumulative probability plot, in that the data do not follow a straight line, as they would if they were in a single lognormal mode. The geometric standard deviations in Table 4 for each process are also too large for single modes.

The MMADs in Table 4 are rather small and do not match the peaks of the mass histogram in Fig. 12 well. This is because the data from both modes were used to fit the straight line extrapolation through the 50th percentile. The coarse fraction flattens the slope of the line, causing it to intersect the 50th percentile at a smaller particle size than expected. If the data from the impactor are split into two modes (Fig. 14), more reasonable MMADs can be calculated from each set of data. See Table 4 and compare it to Table 5, a list of MMADs from other fume researchers. The values for σ_g for the ac-

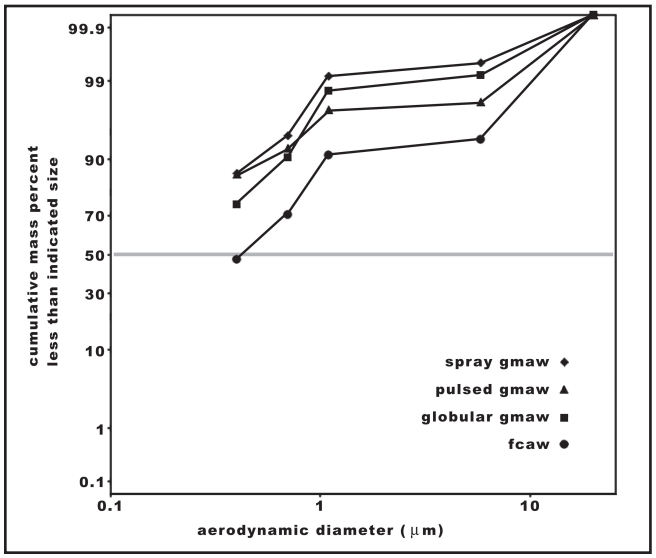

Fig. 13 — Lognormal probability plot of welding fume particles captured with cascade impactor.

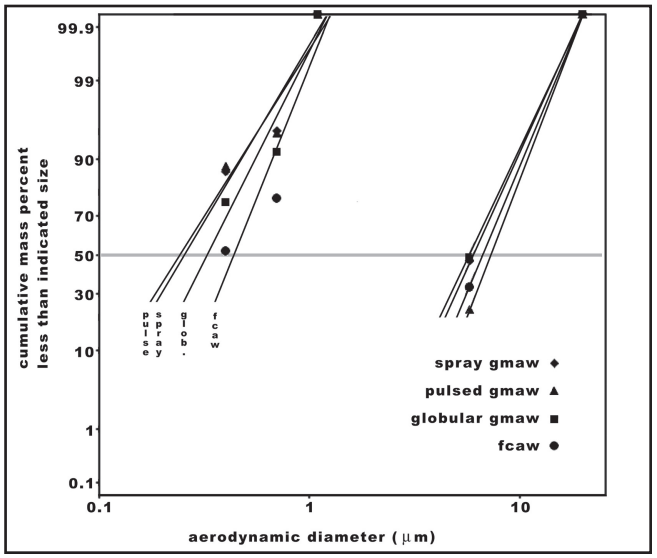

Fig. 14 — Lognormal probability plot of welding fume particles captured with cascade impactor, split into two modes.

Table 5 — Mass Median Aerodynamic Diameter (MMAD) of Welding Fume Particles Calculated from Data Obtained with Cascade Impactors by Other Researchers

Welding Process	MMAD (μm)	Reference
SMAW	0.45 – 0.59 (a)	3
SMAW	0.5 – 0.8	8
SMAW	0.35 (a)	10
SMAW	0.2	11
SMAW	0.3	12
FCAW	0.3	8
FCAW	0.4	9
GMAW	0.25 (a)	3
GMAW	0.2 – 0.4	8
GMAW	0.3	9
GMAW	0.2	11

(a) MMAD reported by the researcher

cumulation mode are now more typical of aerosols, including welding fume (Ref. 4). The MMADs from each run of the various processes were compared to one another with Student's t-test, assuming equal variance. The MMADs of pulsed GMAW and spray GMAW were not significantly different from one another ($t(4) = 1.57$, $p<0.05$ if the MMADs from all stages were compared, $t(4) = 0.98$, $p<0.05$ if only the MMADs from the bottom three stages were compared). It has been speculated (Ref. 20) that pulsed GMAW created differently sized particles than constant current GMAW, but this appears not to be the case. The MMADs of the other processes were significantly different from one another.

The accumulation MMAD of globular GMAW fume may be larger than those of spray or pulsed GMAW fumes because the initial particle concentration is greater, as evidenced by the greater fume formation rate of globular GMAW. Particle concentration speeds agglomeration (Refs. 4, 5, 21), therefore, in the same time (as determined by the distance from welding arc to collection site) larger agglomerates would accumulate from the nucleation mode if the fume formation rate were greater. Jin (Ref. 14) also found that when larger currents were used in GMAW, fume formation rates were greater and welding fume particles were larger. FCAW has a greater fume formation rate than globular GMAW, which explains why FCAW has the largest accumulation MMAD.

The MMAD values for the coarse fraction are not as reliable as those for the accumulation mode, both because there are only two data points, but also because of the 20 μm estimate of the upper cutoff. However, if an upper cutoff of 60 μm were used, the MMADs of the coarse fraction would increase by less than 1 μm, so this may not be an issue.

The distance from weld to collection point naturally affects how many coarse microspatter particles are collected before they fall out of the air (Ref. 16). The distance used in this study was a typical distance from a weld to the welder helmet, but this distance can vary, both in practice and in experiment, which would change the coarse mode MMAD. The same distance was used for each of the welding processes studied, so this may explain the similarities in coarse fraction MMADs for the various processes in this study. See Ref. 5 for more discussion on the size similarities of coarse particles from metallurgical processing.

Since no coarse particles were found on stage F or on the filter (Figs. 5, 6, 10, 11), one can easily say that, by mass, the FCAW fume contains no more than 30% coarse particles (or microspatter), spray GMAW fume has less than 6%, globular GMAW contains less than 10%, and pulsed GMAW fume has less than 8% mi-

crospatter. These data confirm the findings of Zimmer et al. (Ref. 16) who measured the concentration of particles in the coarse size range and concluded that microspatter does not significantly contribute to GMAW fume.

Regardless of the welding parameters that cause different metal transfer modes, less than 10% of the mass of GMAW fume is microspatter (coarse particles). This means that the higher fume formation rates found during globular GMAW, which can be more than double that of spray GMAW, are not caused by an increased fraction of coarse microspatter particles, but from an increase of vapor-condensed particles.

This suggests that there is more evaporation of the electrode in globular GMAW than in spray GMAW. Increased evaporation creates more vapor as well as more spatter, because bursting vapor bubbles create coarse droplets/particles (Ref. 22). Because higher fume formation rates are linked with greater vaporization rates due to increased surface temperatures (Ref. 23), it is proposed that the reason for the observed correlation between fume and spatter rates is not because one causes the other, but rather that both are controlled by the same variables (e.g., surface temperature and electrical current).

Microspatter from FCAW is substantial. This may be because powder from the core of the wire is ejected or because the slag-forming flux is more easily atomized than liquid metal (Ref. 5). So although the FFR of FCAW is much greater than that of GMAW, a smaller percentage of FCAW fume may deposit in the lower lungs.

Conclusion

Impactor separation has shown at least two size modes in the mass distribution of various welding fumes, which is consistent with aerosol theory.

Flux cored arc welding fume contains approximately 30% microspatter by mass. This contributes to the greater fume formation rate of FCAW, but may mean that a smaller fraction of FCAW fume is respirable when compared to fume from GMAW.

Gas metal arc welding fume consists predominately of particle agglomerates smaller than 1 μm. This means that most of the fume is respirable. The size distributions of pulsed GMAW and spray GMAW are not significantly different. Less than 10% of all types of GMAW fume is microspatter. The microspatter fraction does not greatly change with the GMAW parameters, therefore it can be concluded that GMAW FFR does not increase with welding parameters because of greater rates of microspatter formation, but because of increased evaporation of the electrode. Increased FFR may increase the median diameter of the fume particle agglomerates because of increased agglomeration rates.

Knowing how welding parameters affect the size distribution of fume particles helps fume researchers in three ways. First, it adds information to inhalation models of welding fume. Second, it yields insight into what process variables can effectively be changed to reduce the formation of respirable welding particles. Third, since it sheds light on the formation paths of the particles, more rigorous models about fume chemistry can be developed.

Acknowledgment

The funding for this project was provided by a grant from the U.S. Navy, Office of Naval Research.

References

1. Kodas, T. T., and Hampden-Smith, M. J. 1999. *Aerosol Processing of Materials*. New York, N.Y: Wiley-VCH.

2. Willeke, K., and Baron, P. A. (eds.) 1993. *Aerosol Measurement: Principles, Techniques, and Applications*. New York, N.Y.: Van Nostrand Reinhold.

3. Hewett, P. 1995. The particle size distribution, density and specific surface are of welding fumes from SMAW and GMAW mild and stainless steel consumables. *American Industrial Hygiene Association Journal* 56(2): 128–135.

4. Zimmer, A. T., and Biswas, P. 2001. Characterization of the aerosols resulting from arc welding processes. *Journal of Aerosol Science* 32: 933–1008.

5. Jenkins, N. T. 2003. Chemistry of Airborne Particles in Metallurgical Processing. Ph.D. dissertation, Massachusetts Institute of Technology.

6. Deam, R., Bosworth, M., Chen, Z., French, I., Haidar, J., Lowke, J., Norrish, J., Tyagi, V., and Workman, A. 1997. Investigation of fume formation mechanisms in GMAW. *Proceedings of the Technological Developments and Advances for Australian Industry, Int'l Welding and Joining Research Conf.*, Silverwater, Australia, Welding Technology Institute of Australia.

7. Quimby, J. B., and Ulrich, G. D. 1999. Fume formation rates in gas-shielded metal arc welding. *Welding Journal* 78(4): 142–149.

8. Bland, J. (ed.) 1973. *The Welding Environment*. Miami, Fla.: American Welding Society.

9. Heile, R. F., and Hill, D. C. 1975. Particulate fume generation in arc welding processes. *Welding Journal* 54(7): 201-s to 210-s.

10. Berner, V., and Berner, A. 1982. Mass size distributions and elemental frequency distributions of arc welding smokes. *Journal of Aerosol Science* 13: 191–193.

11. Eichhorn, F., and Oldenburg, T. 1986. *Untersuchung der Scheissrauchentstehung beim Schweissen mit mittel- und hochlegierten Zusatzwerkstoffen*. Duesseldorf, BRD, DVS.

12. Stephenson, D., Seshadri, G., and Veranth, J. M. 2003. Workplace exposure to submicron particle mass and number concentrations from manual arc welding of carbon steel. *American Industrial Hygiene Association Journal* 64: 516–521.

13. Sowards, J. W., Lippold, J. C., Dickinson, D. W., and Ramirez, A. J. 2005. Characterization of E6010 and E7018 welding fume. *Proceedings of 7th Int'l Conf. on Trends in Welding Research*, Materials Park, Ohio, ASM International.

14. Jin, Y. 1994. Fume generation from gas metal arc-welding processes. *Staub Reinhaltung der Luft*, 54(2): 67–70.

15. Ren, J. 1997. D*istribution of Particles in Welding Fume*. MS thesis, University of New Hampshire.

16. Zimmer, A. T., Baron, P. A., and Biswas, P. 2002. The influence of operating parameters on number-weighted aerosol size distribution generated from a gas metal arc welding process. *Journal of Aerosol Science* 33(3): 519–531.

17. Chen, B. T. 2005. Characterization of welding fume particles and effect of particle size on lung deposition. *Proceedings of Conference on Health Effects of Welding*, Morgantown, W.Va., NIOSH/West Virginia University.

18. Jenkins N. T., and Eagar, T. W. 2005. Chemical analysis of welding fume particles. *Welding Journal* 84(6): 87-s to 93-s.

19. Thermo Andersen. 2002. Operator Manual: 1 ACFM Nonviable Sample Series 20-800. Thermo Andersen, Symrna, Ga.

20 . Irving, B. 1992. Inverter power sources check fume emissions in GMAW. *Welding Journal* 71(2): 53–57.

21. Friedlander, S. K. 1977. *Smoke, Dust and Haze: Fundamentals of Aerosol Behavior*. New York, N.Y.: Wiley.

22. Jenkins, N. T., Mendez, P. F., and Eagar, T. W. 2005. Effect of arc welding electrode temperature on vapor and fume composition. *Proceedings of 7th Int'l Conf. on Trends in Welding Research*, Materials Park, Ohio: ASM International.

23. Mendez, P., Jenkins, N. T., and Eagar, T. W. 2000. Effect of electrode droplet size on evaporation and fume generation in GMAW. *Proceedings of the Gas Metal Arc Welding for the 21st Century*, Miami, Fla.: American Welding Society.